PROCEEDINGS B

royalsocietypublishing.org/journal/rspb

Research

Cite this article: Kvalnes T, Sæther B-E, Engen S, Roulin A. 2022 Density-dependent selection and the maintenance of colour polymorphism in barn owls. *Proc. R. Soc. B* **289**: 20220296.
https://doi.org/10.1098/rspb.2022.0296

Received: 21 February 2022
Accepted: 5 May 2022

Subject Category:
Evolution

Subject Areas:
evolution, genetics, ecology

Keywords:
population density, individual fitness, natural selection, reproductive value, *Tyto alba*

Author for correspondence:
Thomas Kvalnes
e-mail: thomas.kvalnes@ntnu.no

Electronic supplementary material is available online at https://doi.org/10.6084/m9.figshare.c.5999966.

THE ROYAL SOCIETY PUBLISHING

Density-dependent selection and the maintenance of colour polymorphism in barn owls

Thomas Kvalnes[1], Bernt-Erik Sæther[1], Steinar Engen[2] and Alexandre Roulin[3]

[1]Department of Biology, Centre for Biodiversity Dynamics (CBD), and [2]Department of Mathematical Sciences, Centre for Biodiversity Dynamics (CBD), Norwegian University of Science and Technology (NTNU), Trondheim NO-7491, Norway
[3]Department of Ecology and Evolution, University of Lausanne, Biophore Building, Lausanne CH-1015, Switzerland

TK, 0000-0002-3088-7891; B-ES, 0000-0002-0049-9767; SE, 0000-0001-5661-1925; AR, 0000-0003-1940-6927

The capacity of natural selection to generate adaptive changes is (according to the fundamental theorem of natural selection) proportional to the additive genetic variance in fitness. In spite of its importance for development of new adaptations to a changing environment, processes affecting the magnitude of the genetic variance in fitness-related traits are poorly understood. Here, we show that the red-white colour polymorphism in female barn owls is subject to density-dependent selection at the phenotypic and genotypic level. The diallelic melanocortin-1 receptor gene explained a large amount of the phenotypic variance in reddish coloration in the females ($R^2 = 59.8\%$). Red individuals (RR genotype) were selected for at low densities, while white individuals (WW genotype) were favoured at high densities and were less sensitive to changes in density. We show that this density-dependent selection favours white individuals and predicts fixation of the white allele in this population at longer time scales without immigration or other selective forces. Still, fluctuating population density will cause selection to fluctuate and periodically favour red individuals. These results suggest how balancing selection caused by fluctuations in population density can be a general mechanism affecting the level of additive genetic variance in natural populations.

1. Introduction

One of the most important contributions in evolutionary biology is Fisher's [1] fundamental theorem of natural selection, stating that the partial rate of increase in fitness is equal to its additive genetic variance in fitness [2,3]. This implies that consistent natural selection favouring genotypes of high fitness may deplete the additive genetic variance in fitness [4], reducing the capacity of a population to change genetically from one generation to the next. Still, comparative analyses of heritability and evolvability suggest that there is substantial potential for evolutionary changes in most traits, but also reveal large variation between traits [5,6]. Factors affecting this large variation in additive genetic variance are poorly understood and is a major reason for why evolutionary biologists have found it difficult to develop reliable predictions of evolutionary responses to changes in the environment [7].

Fluctuations in environmental conditions and population density affect the vital rates of natural populations, causing populations to fluctuate in size [8]. The close link between the population growth rate and expected absolute fitness means that feedbacks between population density and adaptive evolution may induce density-dependent selection [9–17]. Then mean fitnesses of different phenotypes and genotypes depends on population density and selection will have both density-dependent and density-independent components [14,16–20]. MacArthur & Wilson [21] introduced the concept of *r*- and *K*-selection, where *r* is the population growth rate in the absence

of density regulation (very small values of N) and K is the carrying capacity of the population. This model proposes that those phenotypes favoured at small population densities are selected against at population sizes close to the carrying capacity [18,21–26]. Theoretical models have shown that this can lead to fluctuating selection around an intermediate value of the phenotype [14,18,19,23–25] (but see Asmussen [27]), which in a fluctuating environment facilitates maintenance of genetic variance. Accordingly, a combination of density-dependent and stabilizing selection in great tits *Parus major* causes the mean clutch size per season to fluctuate around an intermediate optimum maximizing the expected population size [16]. Thus, fluctuations in population size may provide a general agent of selection which also may maintain additive genetic variance in fitness-related characters.

Analyses of colour polymorphisms have been popular study systems in evolutionary biology for a long period of time [28,29]. Such polymorphisms are often determined by one or a few genes of large effect [30–32] and frequently related to variation in individual fitness components [29,33–37]. Importantly, in several natural populations of animals, there exists colour polymorphisms which seems to be relatively stable over time [30,38,39]. This suggests the action of balancing selection, which is any form of natural selection that promote the maintenance of polymorphisms at a higher level than would be expected from genetic drift and mutation rates alone [23,39–42].

Barn owl *Tyto alba* populations harbours a distinct colour polymorphism, where the ventral body parts vary in coloration between individuals from white to dark red and also have a variable number and size of black spots [31,32,43]. Coloration and spottiness are largely heritable [43] and the diallelic melanocortin-1 receptor (*MC1R*) gene has been identified as a gene of large effect [31,32]. The variation in these two traits are to different degrees phenotypically correlated to individual differences in behaviour and to variation in several life-history traits [44–46]. In addition, plumage coloration affects the perception of individuals by predators, conspecifics and prey species such that performance of the individuals may depend on their coloration [29,46,47].

In this study, we examine density-dependent selection on coloration and spottiness in female barn owls in a Swiss study population. Individuals have their phenotype scored for the degree of eumelanic spottiness and reddish pheomelanic coloration, and are genotyped for the *MC1R*-gene. We explore whether balancing selection caused by fluctuations in population size is able to maintain a colour polymorphism at the genetic and phenotypic level. To do this, we apply a new evolutionary maximization principle showing that in populations subject to density regulation evolution tends to maximize the expected population size [14,19].

2. Material and methods

(a) Data collection

The data were collected from 1990 to 2016 in a population of barn owls *Tyto alba* on the plains southwest of lake Neuchâtel in western Switzerland (46°49′ N, 06°56′ E). The birds are sexually mature at age 1 year and mainly breed in nest boxes on farms in the area. Females can lay one or two broods of two to 11 eggs (median clutch size: six eggs) from late February to mid-August and incubate the eggs for approximately 32 days. Nestlings are fed in the nest until they fledge at approximately 55 days of age. The total annual population size (N) of the barn owls ranged from 52 to 187 individuals in the study period with a mean of 113.1 (s.d. = 40; electronic supplementary material, figure A1).

Females were captured at the nest during incubation. Nestlings and any unmarked adults were marked with a numbered metal ring, then blood and feather samples were drawn for DNA. Nestling sex was identified using sex-specific molecular markers (the SPINDLIN-gene [48]), while adult breeding females were recognized based on the presence of a brood patch. Year of birth was known for females marked as nestlings, for other individuals age (in years) was deduced based on moult patterns in coverts and flight feathers. Since 1994, in the plumage for each of m body parts on adult females, the number (ν_m) and mean diameter ($d_m \pm 0.1$ mm) of eumelanic black spots and the degree of reddish pheomelanic coloration (c_m) were recorded. The black spots were assessed within a 60×40 mm (2400 mm^2) frame and the reddish coloration was scored using eight-colour chips ranging from −8 (white) to −1 (dark reddish). The measured body parts were the breast, belly, each flank and each of the undersides of the wings, to account for the differential expression of the traits. For each individual, we standardized the traits to age 1 year old using a mixed-effects model with three age classes (1, 2 and 3+ years old) and random slope and intercept for each individual. Then we calculated the mean spottiness (area of the plumage covered by black spots $= 100 \times (\Sigma_1^m \pi r_m^2 \nu_m/2400)/m$, where $r_m = d_m/2$) and mean colour ($\Sigma_1^m c_m/m$) across the m measured body parts.

In the period 1996–2016, genomic DNA was extracted from blood samples of dried feathers using the DNeasy Tissue and Blood kit or the Biosprint robot (Qiagen, Hombrechtikon, Switzerland). Then the *MC1R* genotype was determined using allelic discrimination. Each individual was genotyped twice using PCR products from independent duplicated runs. Detailed protocols on DNA extraction and genotyping can be found in San-Jose *et al.* [31]. A total of 540 females were genotyped, resulting in 374 WW, 155 WR and 11 RR individuals in our sample. For various reasons, a few females each year were not available for genotyping. In 1996, 20 individuals were not genotyped, but for the years 1997–2016 there were 0 (5 years), 1 (4 years), 3 (2 years), 5 (1 year), 6 (1 year) or 7 (1 year) females that were not genotyped.

We structured the data using pre-breeding census. Hence, age 1 year old was the first age class, survival was recorded as 1 if an individual was alive in the beginning of the next years breeding season (otherwise 0) and reproduction was determined as the number of nestlings which were alive to recruit into the next years breeding population (i.e. the number of recruits). Juvenile (age <1) emigration is common in this population; here, emigrants are treated as locally dead individuals (which reduced the estimated fecundity rates). The recapture rate has previously been estimated as 0.84 for adults in this population [49].

(b) Density-dependent selection

(i) Model

The population vector of an age-structured population is denoted as $\mathbf{n} = (n_1, n_2, \ldots, n_k)^T$, where T denotes matrix transposition, and the total population size $N = \Sigma n_x$ for age classes $x = (1, 2, \ldots, k)$. As we only work with the female subset of the population, we assume that there are always adequate numbers of males present for all females to be mated. In fluctuating environments, the population growth of density regulated age-structured populations is governed by the stochastic projection matrix $\mathbf{L}$ such that $\mathbf{\Delta n = Ln - n}$ [50], where $\mathbf{L}$ in general is a function of $\mathbf{n}$. We now assume that density regulation only act through the total population size such that $\mathbf{L} = \boldsymbol{L}(N)$. For a large population, we

then have $\mathbf{L}(N) = \bar{\mathbf{L}}(N) + \varepsilon$, where $\bar{\mathbf{L}}(N)$ is the expected projection matrix at population size N and ε is an environmental noise term. The non-zero elements of $\bar{\mathbf{L}}(N)$ are the fecundities $f_x(N) = f_x^* F_x(N)$ for all ages in the first row and the survivals $s_x(N) = s_x^* S_x(N)$ for ages 1 to $k-1$ on the subdiagonal. Additionally, one may have $s_k(N)$ in the lower right element $\bar{L}(N)_{k,k}$ if age class k collects all individuals aged $\geq k$. Here, f_x^* and s_x^* are the density-independent vital rates and $F_x(N)$ and $S_x(N)$ are density-dependent functions for fecundity and survival. For logistic density regulation, $F_x(N) = \mathrm{e}^{-a_x N}$ and $S_x(N) = \mathrm{e}^{-b_x N}$, where a_x and b_x measures the sensitivity of the vital rates in age class x to population density.

At the carrying capacity $N = K$, we have the equilibrium projection matrix $\hat{\mathbf{L}} = \bar{\mathbf{L}}(K)$ with growth rate $\lambda = 1$ given by its real dominant eigenvalue. The stable age distribution $\mathbf{u}$ and reproductive values $\mathbf{v}$ at equilibrium are given as the left and right eigenvectors of $\hat{\mathbf{L}}$ scaled to $\Sigma u_x = 1$ and $\Sigma v_x u_x = 1$ [8,51,52]. At equilibrium, when the population has reached its stable age distribution the total reproductive value V of the population equals the carrying capacity, $V = \mathbf{v}\hat{\mathbf{n}} = K$, where $\hat{\mathbf{n}} = K\mathbf{u}$ (electronic supplementary material, appendix 1, 'Dynamics of reproductive values under density-dependence'). The reproductive value v_x is then the expected contribution of an individual of age x to the growth of the equilibrium population [1].

We assume weak density-dependence, such that the population mostly experience small deviations from equilibrium, to allow the reproductive values at N to be approximated by the reproductive values at equilibrium [51]. The annual contribution of individual i in age class x to the population next year can now be defined as [52,53]

$$\Lambda_i = \frac{W_i}{v_x} = \frac{J_i v_{x+1} + B_i v_1/2}{v_x}, \tag{2.1}$$

where Λ_i is the individual fitness, W_i is the individual reproductive value [52], J_i is a dichotomous indicator of survival (1/0), B_i is the number of recruits produced and the v's are age-specific reproductive values at equilibrium. B_i is multiplied by 1/2 to account for sexual reproduction, assuming sex ratio 1 : 1. The scaling by the reproductive value ensure that $\tilde{E}(\Lambda_i) = \Sigma v_i \Lambda_i / \Sigma v_i = \Sigma W_i / \Sigma v_i = (\Delta V + V)/V = \lambda = \mathrm{e}^r$ independent of age at equilibrium [52,53], where λ is the deterministic growth rate and r is the Malthusian parameter. Henceforth, notation with ˜ indicates reproductive value (rv) weighting, as originally proposed by Fisher [1].

Let there be variation among individuals in a fitness related phenotype z. Furthermore, assume weak selection such that changes in z only cause minor changes to the elements of the equilibrium projection matrix $\hat{\mathbf{L}}$ [54,55]. Then the expected fitness of an individual of phenotype z at population size N in environment ε can be written as $\tilde{E}(\Lambda|z, N, \varepsilon) = \mathrm{e}^{\tilde{M}(z,N,\varepsilon)}$, where $\tilde{M}(z, N, \varepsilon)$ is the conditional Malthusian parameter [14,16]. Taking the expectation over the fluctuating environment, we have [14,16]

$$\tilde{E}_\varepsilon \ln(\Lambda|z, N, \varepsilon) = \tilde{m}(z, N) \approx \tilde{r}(z, N) - \frac{1}{2}\sigma_e^2, \tag{2.2}$$

where $\tilde{m}(z, N)$ is the mean Malthusian parameter and $\tilde{r}(z, N)$ is the deterministic growth rate of a population fixed for phenotype z and population size N, and σ_e^2 is the environmental variance [16].

Similarly as Engen *et al.* [14] and Sæther *et al.* [16], we define the model $\tilde{r}(z, N) = \tilde{r}(z) - \tilde{\gamma}(z)g(N)$, where $\tilde{r}(z)$ governs the growth rate as the population size approach zero, $\tilde{\gamma}(z)$ defines the strength of density regulation and $g(N)$ is a function for the form of density regulation. Henceforth, we define $g(N) = N$ for logistic density regulation. In this model, the mean Malthusian fitness is $\bar{m}(\tilde{z}, N) = \bar{s}(\tilde{z}) - \bar{\gamma}(\tilde{z})N$, where $\bar{s}(\tilde{z}) = \bar{r}(\tilde{z}) - 1/2\sigma_e^2$ (the long-run growth rate in the absence of density regulation), $\bar{r}(\tilde{z}) = \Sigma_{i=1}^N \tilde{r}(z)/N$ and $\bar{\gamma}(\tilde{z}) = \Sigma_{i=1}^N \tilde{\gamma}(z)/N$ [14]. With density-dependent selection, the rv-weighted mean phenotype $\tilde{z}$ is expected to evolve towards the value $\tilde{z}_{\mathrm{opt}}$ that maximize the function $Q(\tilde{z}) = \bar{s}(\tilde{z})/\bar{\gamma}(\tilde{z})$, which is the expected value of N [14]. The selection gradient on the phenotype in this model is given by $\nabla\bar{m}(\tilde{z}, N) = \nabla\bar{s}(\tilde{z}) - \nabla\bar{\gamma}(\tilde{z})N$ [14,16,19], where ∇ indicates the derivative with respect to $\tilde{z}$.

Let the variation in the phenotype partly be caused by a diallelic locus, with alleles 1 and 2. The total reproductive value of allele 1 in the population is then $V_1 = \mathbf{v}\mathbf{X}_1$ [54], where $\mathbf{X}_1$ is the column vector for the numbers of allele 1 for each individual and $\mathbf{v}$ is the row vector with the age-specific reproductive values at equilibrium for each individual. Thus, the rv-weighted mean allele frequency $\tilde{p} = V_1/(V_1 + V_2)$. The expected fitness of an individual with genotype kl at population size N in environment ε can be written as $\tilde{E}(\Lambda|kl, N, \varepsilon) = \mathrm{e}^{\tilde{M}(kl,N,\varepsilon)}$. Taking the expectation over the environment, we have

$$\tilde{E}_\varepsilon \ln(\Lambda|kl, N, \varepsilon) = \tilde{m}(kl, N) \approx \tilde{r}(kl, N) - \frac{1}{2}\sigma_e^2, \tag{2.3}$$

where $\tilde{r}(kl, N) = \tilde{r}(kl) - \tilde{\gamma}(kl)N$, and we assume that the environmental variance σ_e^2 is independent of the genotype. Similarly to the phenotypic model, $\tilde{r}(kl)$ governs the growth rate in the absence of density regulation and $\tilde{\gamma}(kl)$ defines the strength of density regulation. We assume that the locus is pleiotropic and affects both the density-independent and the density-dependent component of the Malthusian fitness. Then, following Falconer [56], we can define the genotypic values for each genotype as $(\tilde{a}_r, \tilde{a}_\gamma)$, $(\tilde{d}_r, \tilde{d}_\gamma)$ and $(-\tilde{a}_r, -\tilde{a}_\gamma)$, where $\tilde{a}_r = \tilde{r}(11) - \tilde{r}_0$, $\tilde{a}_\gamma = \tilde{\gamma}(11) - \tilde{\gamma}_0$, $\tilde{d}_r = \tilde{r}(12) - \tilde{r}_0$ and $\tilde{d}_\gamma = \tilde{\gamma}(12) - \tilde{\gamma}_0$. Here, $\tilde{r}_0 = (\tilde{r}(11) + \tilde{r}(22))/2$ and $\tilde{\gamma}_0 = (\tilde{\gamma}(11) + \tilde{\gamma}(22))/2$, i.e. the midpoints between the expectation for components of the growth rate of the homozygotes. The expected mean Malthusian fitness can then be given as

$$\bar{m}(\tilde{p}, N) = \bar{s}(\tilde{p}) - \bar{\gamma}(\tilde{p})N, \tag{2.4}$$

where $\bar{s}(\tilde{p}) = \bar{r}(\tilde{p}) - 1/2\sigma_e^2$, $\bar{r}(\tilde{p}) = \tilde{a}_r(\tilde{p} - \tilde{q}) + 2\tilde{p}\tilde{q}\tilde{d}_r + \tilde{r}_0$, $\bar{\gamma}(\tilde{p}) = \tilde{a}_\gamma(\tilde{p} - \tilde{q}) + 2\tilde{p}\tilde{q}\tilde{d}_\gamma + \tilde{\gamma}_0$ and $\tilde{q} = 1 - \tilde{p}$. Hence, we can define a function $Q(\tilde{p}) = \bar{s}(\tilde{p})/\bar{\gamma}(\tilde{p})$, which is a maximization principle for the evolution of the allele frequency $\tilde{p}$ under density-dependent selection (electronic supplementary material, appendix 1, 'Maximization principle for allele frequency under density-dependent selection'). Adaptive evolution is expected to maximize the Q-function as the population mean allele frequency evolve towards $\tilde{p}_{\mathrm{opt}}$. The selection gradient on allele frequency in this model is given by $\nabla\bar{m}(\tilde{p}, N) = \nabla\bar{s}(\tilde{p}) - \nabla\bar{\gamma}(\tilde{p})N = 2[\tilde{a}_r - \tilde{a}_\gamma N + (\tilde{q} - \tilde{p})(\tilde{d}_r - \tilde{d}_\gamma N)]$, where ∇ indicates the derivative with respect to $\tilde{p}$.

(ii) Estimation

Age classes 8–15 were collapsed to age class 8+ to ensure that there were sufficient numbers of individuals in each age class in the analyses ($n_x \geq 10$). First, we estimated the observed mean projection matrix $\bar{\mathbf{L}}(N)$ by taking the average of annual age-specific survival (J) and recruit production ($B/2$) over years (electronic supplementary material, table A2a). Then to estimate the elements ($\mathbf{s}(N)$, $\mathbf{f}(N)$) of the expected equilibrium projection matrix $\bar{\mathbf{L}}(K)$ we applied separate generalized linear models (GLMs) for survival and recruit production with age categories and $\Delta N/N$ as explanatory variables (electronic supplementary material, table A1). For survival, we fitted a GLM with binomial error distribution and a logit link function, and for fecundity, we fitted a GLM with Poisson error distribution, a log link function, and an offset of ln2 and weights 1/2 to account for sexual reproduction (on average, half of the recruits are females). $E(\Delta N/N | N) = \lambda(N, \phi) - 1$, where ϕ collects all parameters affecting the population growth rate [8]. Hence, we predicted survival and fecundity rates at K from the GLMs by setting $\Delta N/N = 0$

(electronic supplementary material, table A2b). Due to emigration of juveniles, which result in reduced estimates of fecundities in the study population, the growth rate of $\bar{\mathbf{L}}(K)$ was lower than one ($\lambda_K = 0.58$). Accordingly, to obtain a stationary model at K we scaled the recruit production $\mathbf{f}(K)$ by a constant c to obtain $\bar{\mathbf{L}}^*(K)$ (electronic supplementary material, table A2c). The c was estimated by solving the Euler–Lotka equation, $c\sum \lambda(K)^{-x} l_x(K) f_x(K) = 1$, using the Newtons method. Here, $l_x(K) = \prod_{x=1}^{k-1} s_x(K)$ and $\lambda(K) = 1$. Given the equilibrium projection matrix $\bar{\mathbf{L}}^*(K)$, reproductive values ($\mathbf{v}$) and the stable age distribution ($\mathbf{u}$) were estimated as the scaled left and right eigenvector [50,52]. We also estimated reproductive values for all observed $\Delta N/N$ to investigate the difference from the reproductive values at equilibrium (electronic supplementary material, figure A2). There were no evidence for a difference on average between the reproductive values at the observed population densities and the reproductive values at equilibrium (ANOVA: mean difference = -0.0001 ± 0.0043, $F_{7,200} = 1.67$, $p = 0.118$, electronic supplementary material, figure A2). Hence, the reproductive values at equilibrium were good estimates of the expected contributions of the age classes to the future population growth when averaged over N in our population.

We fitted generalized mixed effects models, using the R package *lme4* (v. 1.1-21), with a random intercept for year to estimate the density-dependent and density-independent parameters in our population (equations (2.2) and (2.3)). For each phenotype (z), mean spottiness or mean colour, we define $\tilde{r}(z) = \beta_1 + \beta_2 z + \beta_3 z^2$ to allow a test for an intermediate phenotypic optimum in the growth rate as a function of z and $\tilde{\gamma}(z) = -\beta_4 - \beta_5 z$ to test for a decrease in $\tilde{\gamma}(z)$. The selection gradient on the phenotype with this parameterization is found to be $\nabla\bar{m}(\tilde{z}, N) = \beta_2 + 2\beta_3\tilde{z} + \beta_5 N$ [14]. To ease model convergence, the traits were standardized to a mean of 0 and unit variance prior to analyses (colour: mean = -4.586 ± 0.045, s.d. = 1.412, spottiness: mean = 3.898 ± 0.100, s.d. = 2.560). Parameter estimates were backtransformed and are reported for mean centred traits. Thus, the selection gradients are unscaled. Similarly for the MC1R-genotype, we define $\tilde{r}(kl) = \beta_1 + \beta_2 x_{\mathrm{WR}} + \beta_3 x_{\mathrm{RR}}$ to test for an effect of genotype (kl) on the growth rate and $\tilde{\gamma}(kl) = -\beta_4 - \beta_5 x_{\mathrm{WR}} - \beta_6 x_{\mathrm{RR}}$ to test for a difference in the density-dependence for each genotype. Here, the x_{kl}'s are dummy variables which take the value 1 for individuals of genotype kl (otherwise 0). The selection gradient on the allele frequency $\nabla\bar{m}(\tilde{p}, N) = 2[\tilde{a}_r - \tilde{a}_\gamma N + (\tilde{q} - \tilde{p})(\tilde{d}_r - \tilde{d}_\gamma N)]$ with this parameterization is given by $\tilde{a}_r = (\beta_1 - (2\beta_1 + \beta_3)/2)$, $\tilde{a}_\gamma = -\beta_4 - (-2\beta_4 - \beta_6)/2$, $\tilde{d}_r = (\beta_1 + \beta_2) - (2\beta_1 + \beta_3)/2$ and $\tilde{d}_\gamma = (-\beta_4 - \beta_5) - (-2\beta_4 - \beta_6)/2$.

The model, specified for a given year t, was $\ln\tilde{E}(\Lambda_t) = \mathbf{X}_t\boldsymbol{\beta} + \mathbf{1}_t\mathbf{u}_t$, where $\mathbf{1}$ is a column vector of ones, $\mathbf{u}$ is a normal environmental noise with zero expectation and temporal variance σ_e^2, $\mathbf{X}$ is a design matrix and $\boldsymbol{\beta}$ is a column matrix with the parameters. In the model for a phenotype, $\mathbf{X}$ had column vectors ($\mathbf{1}$, $\mathbf{z}$, $\mathbf{z}^2$, $\mathbf{N}$, $\mathbf{Nz}$) and $\boldsymbol{\beta} = (\beta_1, \beta_2, \beta_3, \beta_4, \beta_5)^T$, while in the model for genotypes, $\mathbf{X}$ had column vectors ($\mathbf{1}$, $\mathbf{x}_{\mathrm{WR}}$, $\mathbf{x}_{\mathrm{RR}}$, $\mathbf{N}$, $\mathbf{Nx}_{\mathrm{WR}}$, $\mathbf{Nx}_{\mathrm{RR}}$) and $\boldsymbol{\beta} = (\beta_1, \beta_2, \beta_3, \beta_4, \beta_5, \beta_6)^T$. Individual fitness, Λ, does not follow any well characterized distribution. Hence, for a record of individual i we define $2W_i^* = 2J_i + B_i$, which takes integer values and may be modelled using Poisson regression with a log-link function. We then define a scaling variable C_i such that $2W_i^* C_i^{-1} = \Lambda_i$ and find that

$$\begin{aligned}\ln\tilde{E}(\Lambda_t) &\equiv \ln\tilde{E}(\mathbf{2W^*}_t\mathbf{C}_t^{-1}) = \mathbf{X}_t\boldsymbol{\beta} + \mathbf{1}\mathbf{u}_t,\\ &\equiv \ln\tilde{E}(\mathbf{2W^*}_t) = \mathbf{X}_t\boldsymbol{\beta} + \ln\mathbf{C}_t + \mathbf{1}\mathbf{u}_t,\end{aligned} \tag{2.5}$$

where $\ln\mathbf{C}_t$ is an offset with parameter value fixed at 1 and the model is fitted with weights $\boldsymbol{\omega}_t = \mathbf{v}_t\mathbf{C}_t^{-1}$, where $\mathbf{v}_t$ are the age-specific reproductive values for each individual in year t.

Migration is an important component of the dynamics in this barn owl population [49]. Hence, we had to estimate the migration rate μ needed to obtain a stable population at the carrying capacity and replace $\bar{s}(\tilde{z})$ and $\bar{s}(\tilde{p})$ by $\bar{s}(\tilde{z}) + \mu$ and $\bar{s}(\tilde{p}) + \mu$ in the expressions for the Q-function and the mean Malthusian fitness $\bar{m}$. The log growth rate at the carrying capacity can be estimated as $\ln\lambda_K - 1/2\sigma_e^2 + \mu = 0$, where λ_K is the deterministic growth rate obtained from the unscaled equilibrium projection matrix $\bar{\mathbf{L}}(K)$. Thus, the migration rate was estimated as $\mu = -ln\lambda_K + 1/2\sigma_e^2$.

The significance of parameter estimates were assessed using likelihood ratio tests, in which twice the difference in log likelihood between two nested models is χ^2-distributed with degrees of freedom (d.f.) equal to $df_1 - df_2$. Parameter estimates are provided with 95% confidence intervals (CI). All analyses were performed in the statistical software R (v. 4.0.5).

3. Results

The MC1R genotype significantly affected the expression of the degree of spottiness (number and size of spots, ANOVA: $F_{2,342} = 13.09$, $p < 0.0001$; electronic supplementary material, figure A3*a*,*b*) and the degree of reddish coloration (ANOVA: $F_{2,526} = 391.10$, $p < 0.0001$; electronic supplementary material, figure A3*c*,*d*). Homozygote RR individuals were less spotted and more red than individuals with the WW genotype, while heterozygote WR individuals were as spotted as RR individuals and intermediate in the degree of reddish coloration (electronic supplementary material, figure A3). Overall the MC1R genotype explained 7.1% of the variation in spottiness and 59.8% of the variation in reddish coloration.

There was clear evidence of density-dependence in the vital rates, with a negative relationship between $\Delta N/N$ (the multiplicative growth rate − 1) and N in the time series (regression: $b = -0.007 \pm 0.002$, $F_{1,24} = 18.48$, $p = 0.0002$; figure 1*a*). The multiplicative growth rate was positively associated with both recruit production ($b = 1.631 \pm 0.171$, $\chi^2 = 89.49$, d.f. = 1, $p < 0.0001$; figure 1*b*; electronic supplementary material, table A1a) and survival ($b = 1.377 \pm 0.158$, $\chi^2 = 84.69$, d.f.=1, $p < 0.0001$; figure 1*c*; electronic supplementary material, table A1b). Thus, both fitness components contributed similarly to changes in growth rates.

(a) Phenotypic selection

There was significant density-dependent selection on the degree of reddish coloration ($\beta_{Nz} = -0.0018$, $\mathrm{CI}_{Nz} = [-0.0035, -0.0001]$, $\chi^2 = 4.2$, d.f. = 1, $p = 0.040$; electronic supplementary material, table A3a, figures 2 and electronic supplementary material, A4), but no significant density-dependent selection on spottiness ($\beta_{Nz} = 0.0011$, $\mathrm{CI}_{Nz} = [-0.0003, 0.0026]$, $\chi^2 = 2.21$, d.f. = 1, $p = 0.137$; electronic supplementary material, table A3b). Red individuals were favoured at low densities, while white individuals were favoured at high densities (figure 2*a*,*c*). The population growth rate generally decreased with increased population density due to density regulation, but white individuals were less sensitive than red individuals to changes in density (figure 2*a*). There was no significant stabilizing selection on the degree of reddish coloration ($\beta_{z^2} = -0.0032$, $\mathrm{CI}_{z^2} = [-0.0475, 0.0394]$, $\chi^2 = 0.02$, d.f. = 1, $P = 0.883$; electronic supplementary material, table A3a). Accordingly, the mean phenotype in the population is expected to move towards white individuals as evolution maximize $Q(\tilde{z})$, the maximum

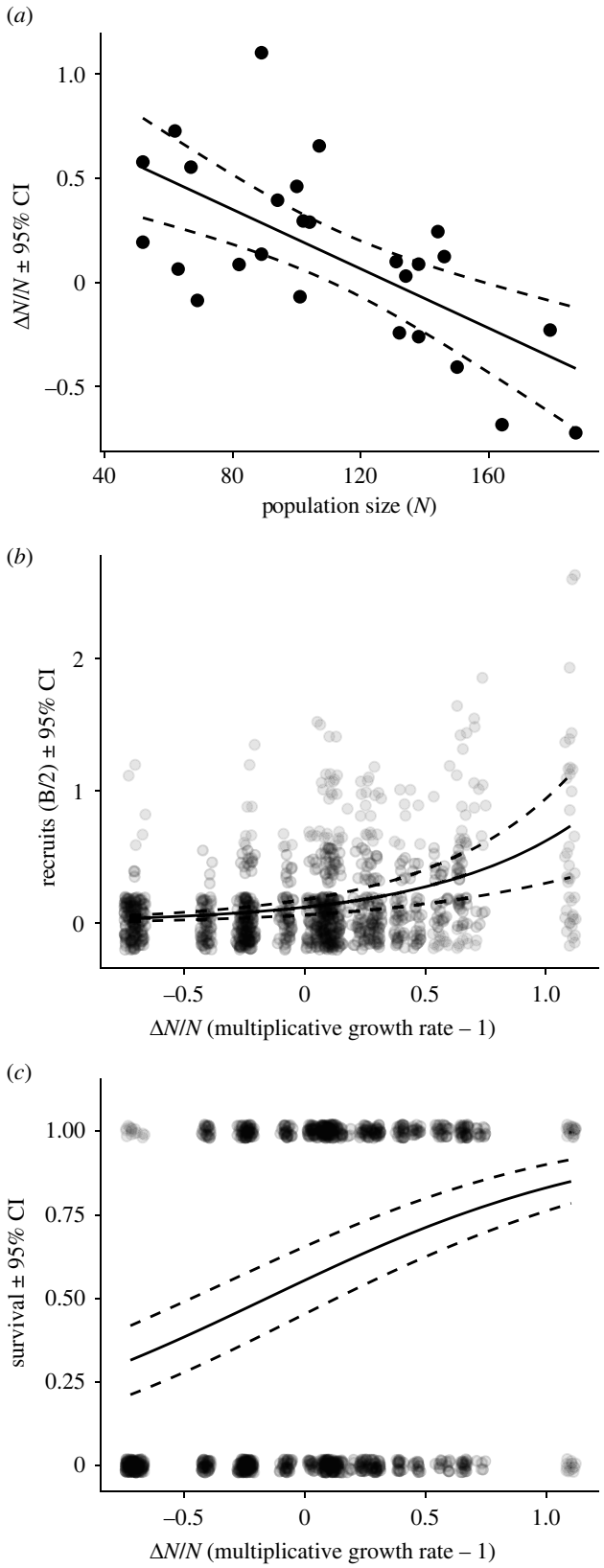

Figure 1. Density-dependence in a time series of (*a*) population size (N), and in individual records of (*b*) recruit production and (*c*) survival in female barn owls in western Switzerland. ΔN equals $N - N_{t+1}$ and $\Delta N/N = \lambda - 1$, where λ is the multiplicative growth rate. Small displacements have been added to the data points in (*b*,*c*) to avoid overlapping and improve visualization. The solid lines are predictions of the relations between the variables from a linear regression (*a*), a Poisson regression (*b*) and a binomial regression (*c*), with dashed lines showing 95% confidence intervals (CI). Predictions of recruit production and survival are given for barn owls in age class three.

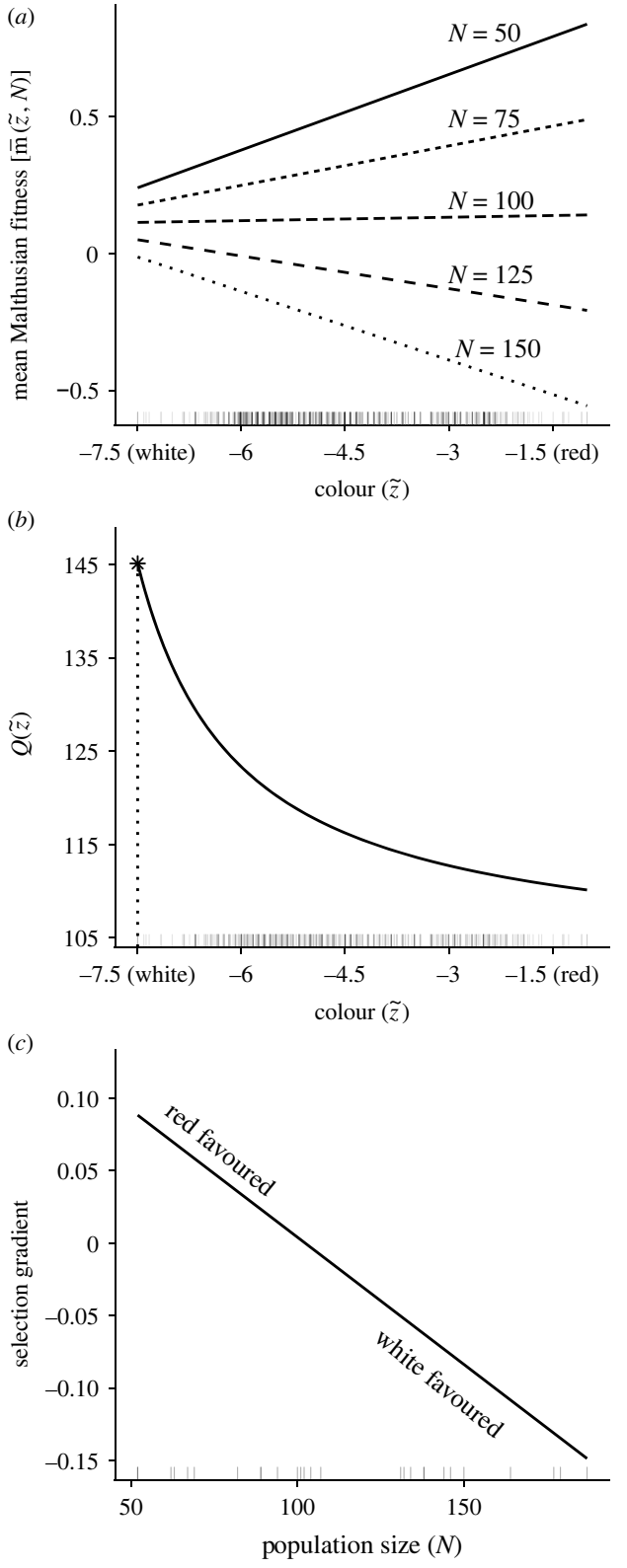

Figure 2. Density-dependent selection on the degree of reddish pheomelanic coloration in female barn owls. (*a*) Estimated mean Malthusian fitness for different phenotypic means $\tilde{z}$ at five different population sizes, ranging from low ($N = 50$) to high ($N = 150$). Red individuals are favoured at low densities, while white individuals are favoured at high densities. (*b*) The estimated $Q(\tilde{z})$-function for the phenotypic mean $\tilde{z}$. Evolution is expected to maximize the Q-function under density-dependent selection. Higher values of $Q(\tilde{z})$ can be interpreted as higher carry capacity. Thus, the population is expected to evolve towards white coloured birds (as indicated by the star and dotted line). (*c*) The relationship between the selection gradient (unscaled) on phenotype and the population size. The effect of migration was accounted for in all panels (see *Estimation* in Materials and methods). Rug plots display individual observations of the degree of reddish coloration (*a*,*b*) and annual population size (*c*).

expected population size as function of the mean phenotype (figure 2*b*).

(b) Genotypic selection

At the genetic level, there was an overall trend for density-dependent selection on the MC1R genotype ($\chi^2 = 4.91$, d.f. = 2, $p = 0.086$; electronic supplementary material, table A4; figure 3; electronic supplementary material, A5). The strength of density regulation was significantly stronger in red individuals (RR genotype) than in white individuals (WW genotype) ($\beta_{Nx_{RR}} = -0.0275$, $CI_{Nx_{RR}} = [-0.0723, -0.0006]$; electronic supplementary material, table A4), such that red individuals again were the most sensitive to changes in population density (figure 3*a*). Similarly to the results on the phenotype, red individuals had higher Malthusian fitness than white individuals at low densities, while white individuals were superior at high densities and had the highest estimated equilibrium population size (figure 3*a*,*c*). Over a narrow range of variation in population size, just below the mean population size ($\bar{N} = 113.1 \pm 7.7$ s.e.), the estimated model show a slight overdominance for mean Malthusian fitness (figure 3*a*). However, the difference between WR and WW individuals was not significant ($\beta_{Nx_{WR}} = -0.0030$, $CI_{Nx_{WR}} = [-0.0084, 0.0024]$, electronic supplementary material, table A4). Accordingly, maximizing the value of $Q(\tilde{p})$ the population was expected to evolve towards fixation of the *W*-allele (figure 3*b*). The strength of selection depended on the population size and became weaker as the allele frequency ($\tilde{p}$) approached 1 (figure 3*c*).

4. Discussion

The dual role of the population growth rate in evolution and ecology means that density-dependent selection can be a particularly direct and important part of the eco-evolutionary dynamics of natural populations [12,14–17,19,20,26,51,57]. Empirically, the study of this process is much more challenging than studying density-dependence and adaptation separately. It requires long-term collection of high-quality data on both population parameters, such as population size and composition, and evolutionary parameters, such as phenotypes and individual fitness. The present study was facilitated by the availability of long-term individual-based level data from an intensively monitored population of barn owls. These owls have a high degree of fidelity to their breeding sites and home range, maintaining similar home ranges from year to year [49]. Thus, population size and composition could be estimated with high accuracy and precision, and individuals that were established in the population could be monitored throughout their life.

The degree of reddish pheomelanic coloration and the MC1R genotype in females were found to be under density-dependent selection in our barn owl population (figures 2 and 3). Directional selection was estimated to be zero at a population size around 100 and shifted between favouring red individuals at low population densities to favouring white individuals at high population density (figures 2 and 3). Thus, fluctuations in population size cause temporal fluctuations in directional selection, where 12 years had very high population size ($N > 120$) and 6 years had very low population size ($N < 80$; see electronic supplementary material, figure A1). Differences in coloration generally affect the perception of individuals by conspecifics, predators and prey

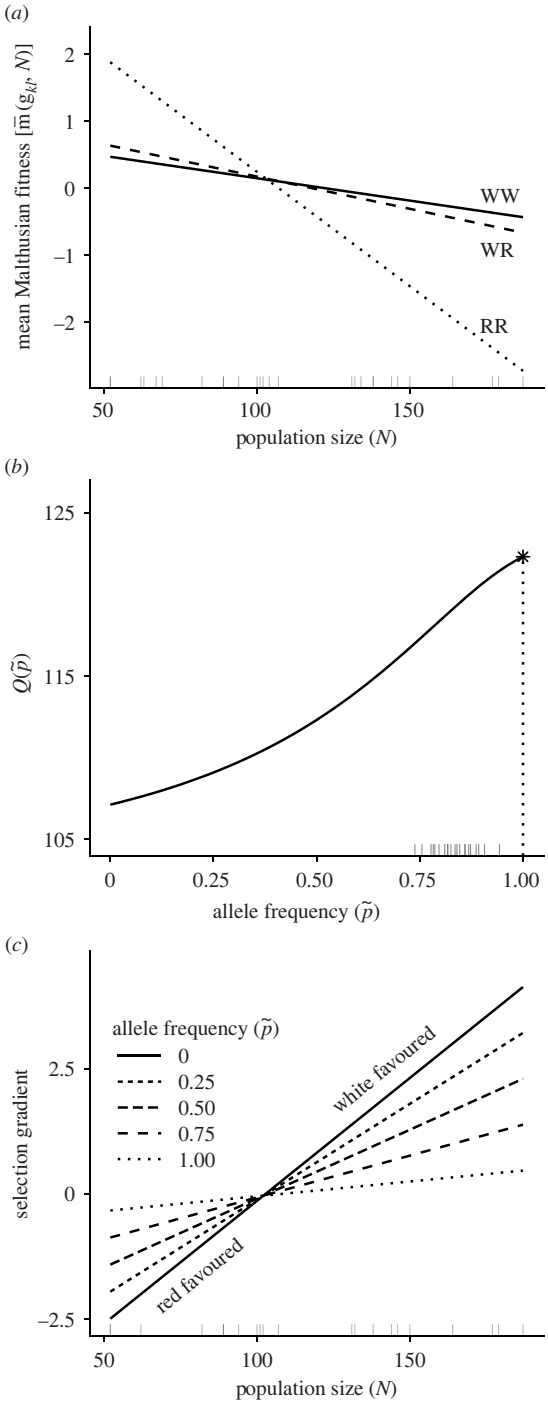

Figure 3. Density-dependent selection on genotype in female barn owls. (*a*) The relationship between the mean Malthusian fitness for each genotype of the melanocortin-1 receptor (*MC1R*) gene and the population size. The red genotype (RR) is shown to be most sensitive to changes in population density, such that WW is favoured at high densities and RR is favoured at low densities. (*b*) The estimated $Q(\tilde{p})$-function for the mean allele frequency $\tilde{p}$. Evolution is expected to maximize the *Q*-function under density-dependent selection. Higher values of *Q* can be interpreted as higher carry capacity. Thus, the population is expected to evolve towards fixation of the white allele (as indicated by the star and dotted line). (*c*) The relationship between the selection gradient and the population size for five different allele frequencies. The effect of migration was accounted for in all panels (see 'Estimation' in Material and methods). Rug plots display observations of annual population size (*a*,*c*) and annual reproductive value weighted average allele frequency (*b*).

[29]. Accordingly, the main prey of barn owls, the common vole *Microtus arvalis*, have been shown to respond with longer freezing times when approached by a white owl

compared to a dark red owl [47]. In addition, the population sizes of predators is likely to have large consequences for their prey species, modifying their abundances, anti-predator behaviours or both [47,58]. This suggests that density-dependent selection can be directly related to variation in coloration through density-dependence in predator–prey interactions. However, melanin-based coloration is generally part of a complex network of correlated traits [29,44,46], which include behaviour, physiology, morphology and life history. In barn owls, the degree of reddish coloration is related to habitat choice, but only weakly correlated to other phenotypes [44]. The size of black spots is on the contrary negatively associated with aggressiveness and the susceptibility to stress [46]. In addition, the correlation between the degree of reddish coloration and spottiness was low among females in this study ($r = 0.027$, $n = 439$). This may explain why we do not find the same pattern of selection on these two traits in this study.

Theoretical and empirical studies have shown that density-dependent selection may facilitate the existence of a stable polymorphism through balancing selection [10,11,14–16,18]. In the present study, density-dependent selection in females was not associated with stabilizing selection on coloration or any clear overdominance at the equilibrium population size (figures 2*c* and 3*c*). Accordingly, in the long term the density-dependent selection was not balancing and in the absence of immigrating red individuals, adaptive evolution was expected to fixate the white (*W*) allele in the population (figures 2*b* and 3*b*; electronic supplementary material, tables A3 and A4). Still, short-term fluctuations in population size could temporally maintain the red-white polymorphism in the barn owls by alternately favouring red and white individuals and make the process of fixating the white allele slow. The analysis in this study is based on the assumption that there is no environmental autocorrelation in the population dynamics [14]. Understanding the effect of any autocorrelated population dynamics on the results of this study and the evolution of coloration would require future analyses. However, Altwegg *et al.* [59] have shown that there are no significant temporal autocorrelation in the different components of survival and reproduction in this barn owl population. In terms of mean Malthusian fitness, the heterozygote WR individuals and the homozygote WW individuals did not significantly differ (see β_2 and β_5 in electronic supplementary material, table A4), suggesting that the *W*-allele was dominant with respect to fitness (figure 3*a*). Such dominance would additionally slow down the rate of evolution towards white individuals as directional selection would become weaker when the allele frequency approached fixation [1].

Mating in the barn owls has been found to be random with respect to the degree of reddish coloration [60]. However, the response to selection on coloration in female barn owls also depends on the pattern of selection in males. Plumage coloration is genetically correlated between the sexes [61] and while males are less red on average, the colour polymorphism in male barn owls is otherwise similar to that in females [31]. Earlier studies have found that reddish coloured males had a higher brood size at fledging than white coloured males [61], while white coloured males had higher recruitment rate than red coloured [62]. Density-dependent selection on the degree of reddish coloration is likely to be similar in both sexes when related to the response in rodent prey to the colour of the owls [47]. Still, at a given population density and allele frequency, with identical selection surfaces, selection will not be equally strong in both sexes due to the difference in the mean coloration between males and females.

Colour polymorphisms in many species display spatial variation [30,37,63], which in several cases are thought to have adaptive value [37,63]. In barn owls, the reddish coloration display a marked latitudinal gradient in North America and Europe, with a preponderance of red individuals in northern and north-eastern populations and white individuals in the southern populations [63,64]. The maintenance of this gradient have been suggested to be due to local adaptation to prey [64] and our results suggest a role for density-dependent selection as a mechanism that affect the variation in coloration also at a spatial scale. For instance, larger environmental stochasticity in population dynamics in northern populations could lower the mean Malthusian growth rate and shift the equilibrium population density in favour of red individuals. Such latitudinal increases in environmental stochasticity has been found in two species of passerine birds [65] and in several species of ducks there were geographical differences in the magnitude of environmental stochasticity [66,67]. Gene flow probably also contributes to the maintenance of the latitudinal gradient in the barn owls, as there is a low genetic differentiation at neutral markers between populations across Europe [68]. In addition, Ducret *et al.* [69] showed that the immigration rate is relatively high for both sexes in our population, but that slightly more of the females are immigrants than the males. With respect to the MC1R genotype, female immigrants were more often heterozygotes than female residents, while male immigrants and residents had similar frequencies of the genotypes [69]. Immigration is positively correlated to emigration and the population size in the study population [49]. In terms of dispersal distance, darker reddish individuals of both sexes have been found to move a longer distance during natal dispersal than more white individuals [45,70]. Breeding dispersal is extremely rare for barn owls in our population [49]. Overall the gene flow, especially due to female immigrants, would increase the effective population size relative to an isolated population and contribute to the maintenance of the R-allele in the local population. This gene flow would probably be quite important as the relatively rare R-allele could easily be lost by chance due to genetic drift. Generally, the impact of genetic drift on evolutionary trajectories increase with decreased population size [71]. Thus, the chance of random loss of the rare allele is increased by population crashes and periods with low population size, such as seen in the years 2009 and 2013 in our barn owl population (see electronic supplementary material, figure A1).

Our results emphasize the importance of considering population density as an agent of selection. Specifically, the maintenance of polymorphisms within populations can be made possible by differences in density-dependent selection and reciprocal gene flow between spatially distributed populations.

Data accessibility. The data and R code for the analyses are available on Dryad (https://doi.org/10.5061/dryad.prr4xgxpd) [72].

Authors' contributions. T.K.: conceptualization, formal analysis, investigation, methodology, software, visualization, writing—original draft, writing—review and editing; B.-E.S.: conceptualization, funding acquisition, resources, writing—review and editing; S.E.: conceptualization, methodology, writing—review and editing; A.R.:

data curation, funding acquisition, project administration, resources, writing—review and editing.

All authors gave final approval for publication and agreed to be held accountable for the work performed therein.

Conflict of interest declaration. We declare that we have no competing interests.

Funding. The study was supported by the Research Council of Norway (SFF-III 223257).

Acknowledgements. We thank all former and current workers from the Roulin's group for the help in sampling and in DNA extraction, and Isabelle Henry Dufresnes for help with management of the long-term barn owl database. This study was authorized by the Veterinary Service of the Canton of Vaud, Switzerland to take blood samples (licence no. 1146) and the Swiss Ornithological station, Sempach, Switzerland, to ring individuals.

References

1. Fisher RA. 1930 *The genetical theory of natural selection*. Oxford, UK: Clarendon Press.
2. Price GR. 1972 Fishers fundamental theorem made clear. *Ann. Hum. Genet.* **36**, 129–140. (doi:10.1111/j.1469-1809.1972.tb00764.x)
3. Ewens WJ. 1989 An interpretation and proof of the fundamental theorem of natural-selection. *Theor. Pop. Biol.* **36**, 167–180. (doi:10.1016/0040-5809(89)90028-2)
4. Bulmer MG. 1971 Effect of selection on genetic variability. *Am. Nat.* **105**, 201–211. (doi:10.1086/282718)
5. Mousseau TA, Roff DA. 1987 Natural-selection and the heritability of fitness components. *Heredity* **59**, 181–197. (doi:10.1038/hdy.1987.113)
6. Hansen TF, Pelabon C, Houle D. 2011 Heritability is not evolvability. *Evol. Biol.* **38**, 258–277. (doi:10.1007/s11692-011-9127-6)
7. Kruuk LEB, Slate J, Wilson AJ. 2008 New answers for old questions: the evolutionary quantitative genetics of wild animal populations. *Annu. Rev. Ecol. Evol. Syst.* **39**, 525–548. (doi:10.1146/annurev.ecolsys.39.110707.173542)
8. Lande R, Engen S, Sæther B-E 2003 *Stochastic population dynamics in ecology and conservation*. Oxford, UK: Oxford University Press.
9. Chitty D. 1960 Population processes in the vole and their relevance to general theory. *Can. J. Zool.* **38**, 99–113. (doi:10.1139/z60-011)
10. Sinervo B, Svensson E, Comendant T. 2000 Density cycles and an offspring quantity and quality game driven by natural selection. *Nature* **406**, 985–988. (doi:10.1038/35023149)
11. Svensson E, Sinervo B. 2000 Experimental excursions on adaptive landscapes: density-dependent selection on egg size. *Evolution* **54**, 1396–1403. (doi:10.1111/j.0014-3820.2000.tb00571.x)
12. Pelletier F, Clutton-Brock T, Pemberton J, Tuljapurkar S, Coulson T. 2007 The evolutionary demography of ecological change: linking trait variation and population growth. *Science* **315**, 1571–1574. (doi:10.1126/science.1139024)
13. Calsbeek R, Cox RM. 2010 Experimentally assessing the relative importance of predation and competition as agents of selection. *Nature* **465**, 613–616. (doi:10.1038/nature09020)
14. Engen S, Lande R, Sæther B-E. 2013 A quantitative genetic model of *r*- and *K*-selection in a fluctuating population. *Am. Nat.* **181**, 725–736. (doi:10.1086/670257)
15. Travis J, Leips J, Rodd FH. 2013 Evolution in population parameters: density-dependent selection or density-dependent fitness? *Am. Nat.* **181**, S9–S20. (doi:10.1086/669970)
16. Sæther B-E, Visser ME, Grøtan V, Engen S. 2016 Evidence for *r*- and *K*-selection in a wild bird population: a reciprocal link between ecology and evolution. *Proc. R. Soc. B* **283**, 20152411. (doi:10.1098/rspb.2015.2411)
17. Kentie R, Clegg SM, Tuljapurkar S, Gaillard JM, Coulson T. 2020 Life-history strategy varies with the strength of competition in a food-limited ungulate population. *Ecol. Lett.* **23**, 811–820. (doi:10.1111/ele.13470)
18. Charlesworth B. 1971 Selection in density-regulated populations. *Ecology* **52**, 469–474. (doi:10.2307/1937629)
19. Lande R, Engen S, Sæther B-E. 2009 An evolutionary maximum principle for density-dependent population dynamics in a fluctuating environment. *Phil. Trans. R. Soc. B* **364**, 1511–1518. (doi:10.1098/rstb.2009.0017)
20. Reznick DN *et al.* 2019 Eco-evolutionary feedbacks predict the time course of rapid life-history evolution. *Am. Nat.* **194**, 671–692. (doi:10.1086/705380)
21. MacArthur RH, Wilson EO 1967 *The theory of island biogeography*. Monographs in Population Biology. Princeton, NJ: Princeton University Press.
22. Pianka ER. 1970 On *r*- and *K*-selection. *Am. Nat.* **104**, 592–597. (doi:10.1086/282697)
23. Roughgarden J. 1971 Density-dependent natural selection. *Ecology* **52**, 453–468. (doi:10.2307/1937628)
24. Clarke B. 1972 Density-dependent selection. *Am. Nat.* **106**, 1–13. (doi:10.1086/282747)
25. Boyce MS. 1984 Restitution of *r*-selection and *K*-selection as a model of density-dependent natural selection. *Annu. Rev. Ecol. Syst.* **15**, 427–447. (doi:10.1146/annurev.ecolsys.15.1.427)
26. Reznick D, Bryant MJ, Bashey F. 2002 *r*- and *K*-selection revisited: the role of population regulation in life-history evolution. *Ecology* **83**, 1509–1520. (doi:10.2307/3071970)
27. Asmussen MA, Feldman MW. 1977 Density dependent selection 1: stable feasible equilibrium may not be attainable. *J. Theor. Biol.* **64**, 603–618. (doi:10.1016/0022-5193(77)90263-6)
28. Ford EB 1964 *Ecological genetics*. London, UK: Methuen and Co.
29. Cuthill IC *et al.* 2017 The biology of color. *Science* **357**, eaan0221. (doi:10.1126/science.aan0221)
30. Steiner CC, Weber JN, Hoekstra HE. 2007 Adaptive variation in beach mice produced by two interacting pigmentation genes. *PLoS Biol.* **5**, 1880–1889. (doi:10.1371/journal.pbio.0050219)
31. San-Jose LM, Ducrest AL, Ducret V, Beziers P, Simon C, Wakamatsu K, Roulin A. 2015 Effect of the MC1R gene on sexual dimorphism in melanin-based colorations. *Mol. Ecol.* **24**, 2794–2808. (doi:10.1111/mec.13193)
32. San-Jose LM, Ducrest AL, Ducret V, Simon C, Richter H, Wakamatsu K, Roulin A. 2017 MC1R variants affect the expression of melanocortin and melanogenic genes and the association between melanocortin genes and coloration. *Mol. Ecol.* **26**, 259–276. (doi:10.1111/mec.13861)
33. Kaufman DW. 1974 Adaptive coloration in *Peromyscus polionotus*: experimental selection by owls. *J. Mammal.* **55**, 271–283. (doi:10.2307/1378997)
34. Brommer JE, Ahola K, Karstinen T. 2005 The colour of fitness: plumage coloration and lifetime reproductive success in the tawny owl. *Proc. R. Soc. B* **272**, 935–940. (doi:10.1098/rspb.2005.3052)
35. Calsbeek R, Buermann W, Smith TB. 2009 Parallel shifts in ecology and natural selection in an island lizard. *BMC Evol. Biol.* **9**, 3. (doi:10.1186/1471-2148-9-3)
36. Roulin A. 2016 Evolutionary trade-off between naturally- and sexually-selected melanin-based colour traits in worldwide barn owls and allies. *Biol. J. Linn. Soc.* **119**, 455–476. (doi:10.1111/bij.12828)
37. Farallo VR, Forstner MRJ. 2012 Predation and the maintenance of color polymorphism in a habitat specialist squamate. *PLoS ONE* **7**, e30316. (doi:10.1371/journal.pone.0030316)
38. Karell P, Ahola K, Karstinen T, Valkama J, Brommer JE. 2011 Climate change drives microevolution in a wild bird. *Nat. Commun.* **2**, 208. (doi:10.1038/ncomms1213)
39. Hedrick PW, Stahler DR, Dekker D. 2014 Heterozygote advantage in a finite population: black color in wolves. *J. Hered.* **105**, 457–465. (doi:10.1093/jhered/esu024)
40. Prout T. 1968 Sufficient conditions for multiple niche polymorphism. *Am. Nat.* **102**, 493–496. (doi:10.1086/282562)
41. Felsenstein J. 1976 Theoretical population genetics of variable selection and migration. *Annu. Rev.*

Genet. **10**, 253–280. (doi:10.1146/annurev.ge.10.120176.001345)

42. Asmussen MA, Basnayake E. 1990 Frequency-dependent selection: the high potential for permanent genetic variation in the diallelic, pairwise interaction model. *Genetics* **125**, 215–230. (doi:10.1093/genetics/125.1.215)
43. Roulin A, Richner H, Ducrest AL. 1998 Genetic, environmental, and condition-dependent effects on female and male ornamentation in the barn owl *Tyto alba*. *Evolution* **52**, 1451–1460. (doi:10.2307/2411314)
44. Dreiss AN, Antoniazza S, Burri R, Fumagalli L, Sonnay C, Frey C, Goudet J, Roulin A. 2012 Local adaptation and matching habitat choice in female barn owls with respect to melanic coloration. *J. Evol. Biol.* **25**, 103–114. (doi:10.1111/j.1420-9101.2011.02407.x)
45. van den Brink V, Dreiss AN, Roulin A. 2012 Melanin-based coloration predicts natal dispersal in the barn owl, *Tyto alba*. *Anim. Behav.* **84**, 805–812. (doi:10.1016/j.anbehav.2012.07.001)
46. van den Brink V, Dolivo V, Falourd X, Dreiss AN, Roulin A. 2012 Melanic color-dependent antipredator behavior strategies in barn owl nestlings. *Behav. Ecol.* **23**, 473–480. (doi:10.1093/beheco/arr213)
47. San-Jose LM *et al.* 2019 Differential fitness effects of moonlight on plumage colour morphs in barn owls. *Nat. Ecol. Evol.* **3**, 1331–1340. (doi:10.1038/s41559-019-0967-2)
48. Py I, Ducrest AL, Duvoisin N, Fumagalli L, Roulin A. 2006 Ultraviolet reflectance in a melanin-based plumage trait is heritable. *Evol. Ecol. Res.* **8**, 483–491.
49. Altwegg R, Roulin A, Kestenholz M, Jenni L. 2003 Variation and covariation in survival, dispersal, and population size in barn owls *Tyto alba*. *J. Anim. Ecol.* **72**, 391–399. (doi:10.1046/j.1365-2656.2003.00706.x)
50. Caswell H 2001 *Matrix population models: construction, analysis, and interpretation*, 2nd edn. Sunderland, MA: Sinauer Associates.
51. Lande R, Engen S, Sæther B-E. 2017 Evolution of stochastic demography with life history tradeoffs in density-dependent age-structured populations. *Proc. Natl. Acad. Sci. USA* **114**, 11 582–11 590. (doi:10.1073/pnas.1710679114)
52. Engen S, Lande R, Sæther B-E, Dobson SF. 2009 Reproductive value and the stochastic demography of age-structured populations. *Am. Nat.* **174**, 795–804. (doi:10.1086/647930)
53. Engen S, Kvalnes T, Sæther B-E. 2014 Estimating phenotypic selection in age-structured populations by removing transient fluctuations. *Evolution* **68**, 2509–2523. (doi:10.1111/evo.12456)
54. Engen S, Lande R, Sæther B-E. 2009 Reproductive value and fluctuating selection in an age-structured population. *Genetics* **183**, 629–637. (doi:10.1534/genetics.109.105841)
55. Engen S, Lande R, Sæther B-E. 2011 Evolution of a plastic quantitative trait in an age-structured population in a fluctuating environment. *Evolution* **65**, 2893–2906. (doi:10.1111/j.1558-5646.2011.01342.x)
56. Falconer DS 1960 *Introduction to quantitative genetics*. Edinburgh, UK: Oliver & Boyd.
57. Engen S, Wright J, Araya-Ajoy YG, Sæther B-E. 2020 Phenotypic evolution in stochastic environments: The contribution of frequency- and density-dependent selection. *Evolution* **74**, 1923–1941. (doi:10.1111/evo.14058)
58. Krebs CJ, Boutin S, Boonstra R, Sinclair ARE, Smith JNM, Dale MRT, Martin K, Turkington R. 1995 Impact of food and predation on the snowshoe hare cycle. *Science* **269**, 1112–1115. (doi:10.1126/science.269.5227.1112)
59. Altwegg R, Schaub M, Roulin A. 2007 Age-specific fitness components and their temporal variation in the barn owl. *Am. Nat.* **169**, 47–61. (doi:10.1086/510215)
60. Roulin A. 1999 Nonrandom pairing by male barn owls (*Tyto alba*) with respect to a female plumage trait. *Behav. Ecol.* **10**, 688–695. (doi:10.1093/beheco/10.6.688)
61. Roulin A, Dijkstra C, Riols C, Ducrest AL. 2001 Female- and male-specific signals of quality in the barn owl. *J. Evol. Biol.* **14**, 255–266. (doi:10.1046/j.1420-9101.2001.00274.x)
62. Roulin A, Altwegg R. 2007 Breeding rate is associated with pheomelanism in male and with eumelanism in female barn owls. *Behav. Ecol.* **18**, 563–570. (doi:10.1093/beheco/arm015)
63. Roulin A, Randin C. 2015 Gloger's rule in North American barn owls. *Auk* **132**, 321–332. (doi:10.1642/Auk-14-167.1)
64. Burri R, Antoniazza S, Gaigher A, Ducrest AL, Simon C, Network EBO, Fumagalli L, Goudet J, Roulin A. 2016 The genetic basis of color-related local adaptation in a ring-like colonization around the mediterranean. *Evolution* **70**, 140–153. (doi:10.1111/evo.12824)
65. Sæther B-E *et al.* 2003 Climate variation and regional gradients in population dynamics of two hole-nesting passerines. *Proc. R. Soc. Lond. B* **270**, 2397–2404. (doi:10.1098/rspb.2003.2499)
66. Sæther B-E, Lillegard M, Grøtan V, Drever MC, Engen S, Nudds TD, Podruzny KM. 2008 Geographical gradients in the population dynamics of North American prairie ducks. *J. Anim. Ecol.* **77**, 869–882. (doi:10.1111/j.1365-2656.2008.01424.x)
67. Feldman RE, Anderson MG, Howerter D, Murray DL. 2015 Where does environmental stochasticity most influence population dynamics? An assessment along a regional core-periphery gradient for prairie breeding ducks. *Glob. Ecol. Biogeogr.* **24**, 896–904. (doi:10.1111/geb.12323)
68. Antoniazza S, Burri R, Fumagalli L, Goudet J, Roulin A. 2010 Local adaptation maintains clinal variation in melanin-based coloration of european barn owls (*Tyto alba*). *Evolution* **64**, 1944–1954. (doi:10.1111/j.1558-5646.2010.00969.x)
69. Ducret V, Schaub M, Goudet J, Roulin A. 2018 Female-biased dispersal and non-random gene flow of MC1R variants do not result in a migration load in barn owls. *Heredity* **122**, 305–314. (doi:10.1038/s41437-018-0115-9)
70. Roulin A. 2013 Ring recoveries of dead birds confirm that darker pheomelanic barn owls disperse longer distances. *J. Ornithol.* **154**, 871–874. (doi:10.1007/s10336-013-0949-0)
71. Lande R. 1985 Expected time for random genetic drift of a population between stable phenotypic states. *Proc. Natl. Acad. Sci. USA* **82**, 7641–7645. (doi:10.1073/pnas.82.22.7641)
72. Kvalnes T, Sæther B-E, Engen S, Roulin A. 2022 Density-dependent selection and the maintenance of colour polymorphism in barn owls. Dryad Digital Repository. (doi:10.1098/rspb.2022.0296)